

LETTER TO THE EDITOR

The radio delay of the exceptional 3C 454.3 outburst**Follow-up WEBT observations in 2005–2006²**

M. Villata¹, C. M. Raiteri¹, M. F. Aller², U. Bach^{1,3}, M. A. Ibrahimov⁴, Y. Y. Kovalev^{3,5,6}, O. M. Kurtanidze^{7,8,9}, V. M. Larionov^{10,11}, C.-U. Lee¹², P. Leto¹³, A. Lähteenmäki¹⁴, K. Nilsson¹⁵, T. Pursimo¹⁶, J. A. Ros¹⁷, N. Sumitomo¹⁸, A. Volvach¹⁹, H. D. Aller², A. Arai¹⁸, C. S. Buemi²⁰, J. M. Coloma¹⁷, V. T. Doroshenko²¹, Yu. S. Efimov²², L. Fuhrmann^{1,23,3}, V. A. Hagen-Thorn^{10,11}, M. Kamada¹⁸, M. Katsuura¹⁸, T. Konstantinova¹⁰, E. Kopatskaya¹⁰, D. Kotaka¹⁸, Yu. A. Kovalev⁵, M. Kurosaki¹⁸, L. Lanteri¹, L. Larionova¹⁰, M. G. Mingaliev²⁴, S. Mizoguchi¹⁸, K. Nakamura¹⁸, M. G. Nikolashvili⁷, S. Nishiyama¹⁸, K. Sadakane¹⁸, S. G. Sergeev²², L. A. Sigua⁷, A. Sillanpää¹⁵, R. L. Smart¹, L. O. Takalo¹⁵, K. Tanaka¹⁸, M. Tornikoski¹⁴, C. Trigilio²⁰, and G. Umana²⁰

¹ INAF, Osservatorio Astronomico di Torino, Italy
e-mail: villata@oato.inaf.it

² Department of Astronomy, University of Michigan, MI, USA

³ Max-Planck-Institut für Radioastronomie, Germany

⁴ Ulugh Beg Astronomical Institute, Academy of Sciences of Uzbekistan, Uzbekistan

⁵ Astro Space Center of Lebedev Physical Institute, Russia

⁶ National Radio Astronomy Observatory, Green Bank, WV, USA

⁷ Abastumani Astrophysical Observatory, Georgia

⁸ Astrophysikalisches Institut Potsdam, Germany

⁹ Landessternwarte Heidelberg-Königstuhl, Germany

¹⁰ Astronomical Institute, St.-Petersburg State University, Russia

¹¹ Isaac Newton Institute of Chile, St.-Petersburg Branch

¹² Korea Astronomy and Space Science Institute, South Korea

¹³ INAF, Istituto di Radioastronomia Sezione di Noto, Italy

¹⁴ Metsähovi Radio Observatory, Helsinki University of Technology, Finland

¹⁵ Tuorla Observatory, Finland

¹⁶ Nordic Optical Telescope, Roque de los Muchachos Astronomical Observatory, TF, Spain

¹⁷ Agrupació Astronòmica de Sabadell, Spain

¹⁸ Astronomical Institute, Osaka Kyoiku University, Japan

¹⁹ Radio Astronomy Laboratory of Crimean Astrophysical Observatory, Ukraine

²⁰ INAF, Osservatorio Astrofisico di Catania, Italy

²¹ Moscow State University, Russia

²² Crimean Astrophysical Observatory, Ukraine

²³ Dipartimento di Fisica e Osservatorio Astronomico, Università di Perugia, Italy

²⁴ Special Astrophysical Observatory, Russia

ABSTRACT

Context. In spring 2005 the blazar 3C 454.3 was observed in an unprecedented bright state from the near-IR to the hard X-ray frequencies. A mm outburst peaked in June–July 2005, and it was followed by a flux increase at high radio frequencies.

Aims. In this paper we report on multifrequency monitoring by the WEBT aimed at following the further evolution of the outburst in detail. In particular, we investigate the expected correlation and time delays between the optical and radio emissions in order to derive information on the variability mechanisms and jet structure.

Methods. A comparison among the light curves at different frequencies is performed by means of visual inspection and discrete correlation function, and the results are interpreted with a simple model taking into account Doppler factor variations of geometric origin.

Results. The high-frequency radio light curves show a huge outburst starting during the dimming phase of the optical one and lasting more than 1 year. The first phase is characterized by a slow flux increase, while in early 2006 a major flare is observed. The lower-frequency radio light curves show a progressively delayed and fainter event, which disappears below 8 GHz. We suggest that the radio major peak is not physically connected with the spring 2005 optical one, but it is actually correlated with a minor optical flare observed in October–November 2005. This interpretation involves both an intrinsic and a geometric mechanism. The former is represented by disturbances travelling down the emitting jet, the latter being due to the curved-jet motion, with the consequent differential changes of viewing angles of the different emitting regions.

Key words. galaxies: active – galaxies: quasars: general – galaxies: individual: 3C 454.3 – galaxies: jets

1. Introduction

In May 2005 the quasar-type blazar 3C 454.3 (2251+158) was observed in an unprecedented luminous state from near-IR to hard X-ray frequencies. A big observing effort was spent to follow the outburst, involving both ground-based and space instruments (Fuhrmann et al., 2006; Giommi et al., 2006; Pian et al., 2006; Villata et al., 2006). In particular, a large multiwavelength campaign was organized by the Whole Earth Blazar Telescope (WEBT)¹, whose first results, up to September 2005, were reported and analysed by Villata et al. (2006). A huge mm outburst followed the optical one, peaking in June–July 2005. In the meantime the high-frequency (43–37 GHz) radio flux started to increase. VLBA observations at 43 GHz during the summer confirmed the brightening of the radio core and showed an increasing polarization.

Follow-up radio-to-optical observations by the WEBT continued until the end of the optical observing season, while a new campaign including three pointings by the XMM-Newton satellite started just after and it is still ongoing. In this paper we present part of these new observations with the aim of studying the correlation between the radio and optical emissions.

2. Observations and analysis

2.1. Optical and radio light curves

In the top panel of Fig. 1 we show the *R*-band data taken by the WEBT from June 2004 to January 2006; grey dots refer to data already published in Villata et al. (2006), while red dots represent the new data collected for this paper. The rightmost point at JD = 2453888.7 (June 2, 2006) indicates the low optical level at which the source was found after the 2006 solar conjunction. These new optical data were taken at the Osaka Kyoiku, Mt. Maidanak, Abastumani, Crimean, Torino, Sabadell, Roque de los Muchachos (KVA and NOT), and Mt. Lemmon Observatories. In the same panel the 43 GHz radio data from June 2004 to the end of August 2006 are shown as black dots together with a cubic spline interpolation through the 15-day binned light curve (blue line). Analogously, the following four panels display data and corresponding splines at 37, 22, 14.5, and 8 GHz. The points after JD = 2453644.5 (end of September 2005) represent new data. They were acquired at the Crimean (RT-22), Medicina, Metsähovi, Noto, SAO RAS (RATAN-600), and UMRAO Radio Observatories. Measurements from the VLA/VLBA Polarization Calibration Database² are also used.

In the *R*-band flux-density light curve one can recognize the rather slow rising phase of the outburst started around JD = 2453250, followed by a period of missing data because of the 2005 solar conjunction. After this, an unprecedently high flux density was observed, rapidly decreasing towards the end of the outburst, which can be located around JD = 2453620. The total outburst duration was thus about 1 year.

The 43 GHz light curve shows a double-humped outburst starting about 250 days after the optical one, and representing the brightest event thus far recorded for this object at high radio frequencies (see the historical light curves in Villata et al. 2006). The first hump (JD \sim 2453500–2453750) is broader and lower,

Send offprint requests to: M. Villata

* For questions regarding the availability of the data presented in this paper, please contact Massimo Villata (villata@oato.inaf.it).

¹ <http://www.to.astro.it/blazars/webt/>

see e.g. Villata et al. (2004a,b); Raiteri et al. (2005, 2006).

² <http://www.vla.nrao.edu/astro/calib/polar/>

reaching at most \sim 14 Jy, while the second hump is more peaked, with a maximum of \sim 20 Jy. The whole event lasted a bit more than 400 days and, at first sight, it seems to mimic well the observed slow rise and fast drop of the optical outburst, with a lag of 250–300 days.

The 37 GHz flux density behaviour is similar, with the main difference that the first hump is substituted by a quasi-monotonic increase, which becomes flatter before the steep rise leading to the maximum peak. This is even higher (\sim 22 Jy) than the 43 GHz one. The dates of start, peak, and end of the event seem to be practically identical to the previous ones.

In the other radio light curves, one can see similar features. However, going towards lower frequencies, the variability amplitude becomes smaller and smaller, while the starting point of the outburst, and to a much less extent also the peak, are more and more delayed. In the 11 GHz light curve (not shown in the figure) the outburst is still clearly observed, with a maximum flux density increase of more than 20%, while at 8 GHz the event is reduced to a barely visible \sim 10% flux density enhancement, which begins about 200 days later than the highest-frequencies one. The 5 GHz light curve (not shown in the figure) is almost completely flat, or even slightly decreasing, in the corresponding period.

2.2. Cross-correlation between radio light curves

In the following, we analyse the time lags mentioned above by means of the discrete correlation function (DCF; Edelson & Krolik 1988; Hufnagel & Bregman 1992). We first investigate the delays among the starting points of the outburst at the different radio wavelengths. To do this, we restrict the calculation to the period before the rise to the maximum peak, to avoid its strong imprint.

The DCF computed on this pre-maximum period (JD \leq 2453750) indicates a delay of the 37 GHz starting point with respect to the 43 GHz one of 5 days³. The DCF between the 37 and 22 GHz light curves shows two equivalent maxima; the first and broader one suggests a mean time lag of 25 days, while the second one indicates a 95 day delay. Finally, the 14.5 GHz outburst would start 160 days later than the 37 GHz one.

Now we consider the whole 815 day period shown in Fig. 1; consequently, the DCF results will be dominated by the presence of the peaks. The DCF applied to the spline interpolations leads to the same results as when using the original data points; hence, in Fig. 2 we show the less noisy cross-correlations between splines. As one can see, the radio emissions from 43 to 14.5 GHz are all well correlated. While no evident lag is present between the 43 and 37 GHz peaks (blue filled circles), the 22 GHz peak is delayed by 10 days (green empty circles), and 40 days separate the 14.5 GHz event from the 37 GHz one (red filled circles).

The progressive delays of the outburst starting points can be interpreted in terms of a disturbance travelling down the jet through more and more transparent emitting regions. In this view, the above results suggest that in the observer's frame the jet becomes transparent quasi-simultaneously at 43 and 37 GHz.

³ Time lags are determined by taking the centroid of the DCF peaks (see e.g. Peterson, 2001; Raiteri et al., 2003). A precise estimate of the uncertainty for the time lags is not easy, depending on the method used and parameters adopted. However, through Monte Carlo simulations, we found typical values around 5 days for almost all the time delays reported in this paper, but for the more uncertain lags of the outburst starting points at 22 and 14.5 GHz, having uncertainties of \sim 10–20 days.

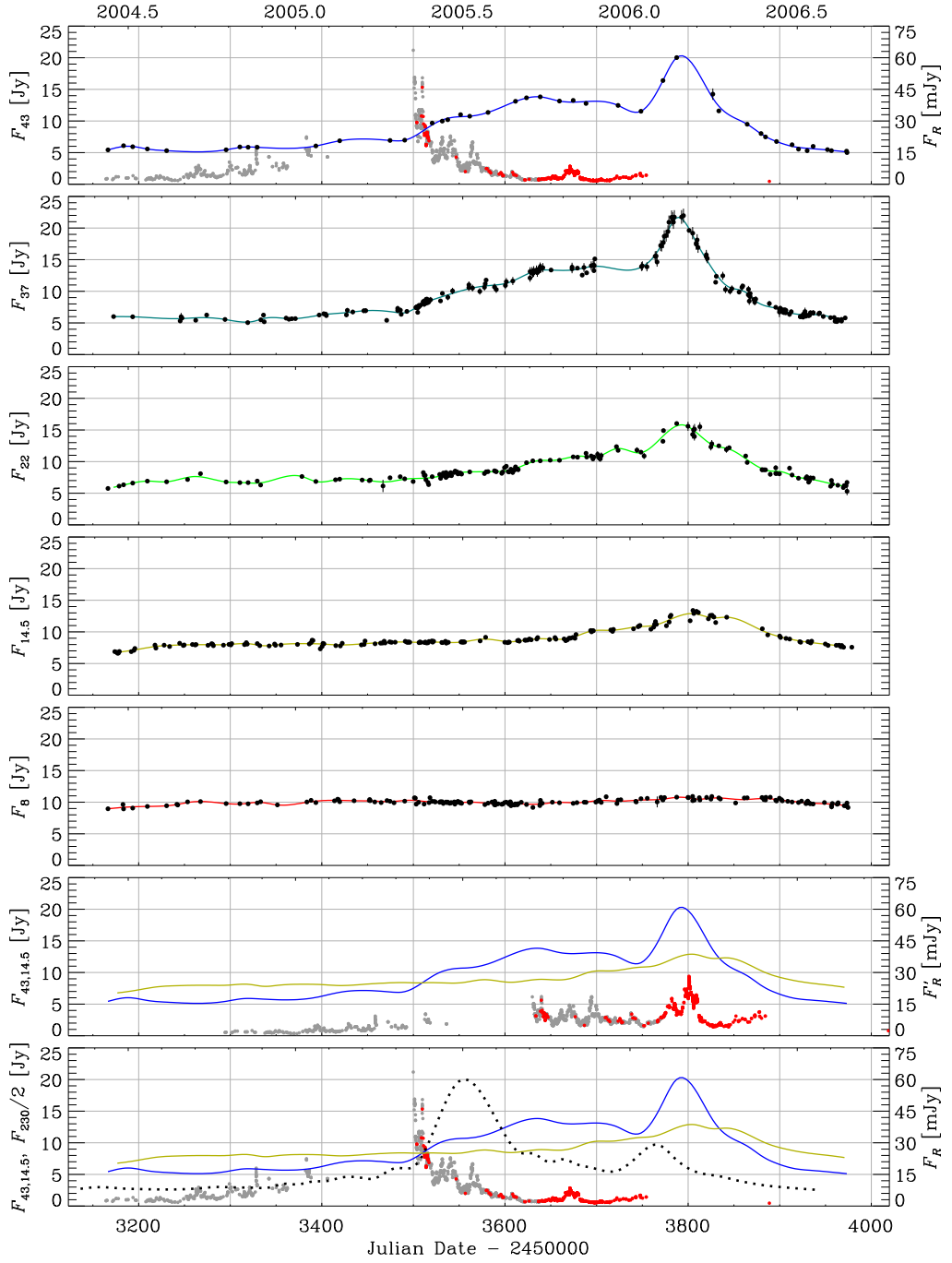


Fig. 1. Optical and radio light curves of 3C 454.3 from June 2004 to the end of August 2006. In the top and bottom panels the grey dots represent R -band flux densities from Villata et al. (2006), while red dots display new data. In the last but one panel the R -band light curve (grey and red dots) has been modified by “rebeaming” and time shifting, as explained in the text. The first five panels from top show the 43, 37, 22, 14.5, and 8 GHz light curves along with their 15-day binned cubic spline interpolations. The 43 and 14.5 GHz splines are also reported in the last two panels for a comparison with the other light curves. In the bottom panel a sketch of the predicted 1 mm (230 GHz) light curve is also plotted as a dotted line.

Then, some tens of days are needed to reach the region where it is barely transparent also to the 22 GHz emission, which however is maximally radiated about 100 days after the highest frequencies. A couple of months later also the 14.5 GHz emission can escape the jet.

However, in a simple model, one would expect that also the peaks and subsequent dimming phases present comparable delays, while here they are found to be much shorter. Actually, it

seems that something occurred, making the outburst stop quasi-simultaneously at all radio frequencies.

2.3. Cross-correlation between optical and radio light curves

As noticed in Sect. 2.1 from a visual inspection of Fig. 1, the optical and 43 GHz light curves seem to nicely correlate with a 250–300 day radio lag. Indeed, the cross-correlation analysis yields a 275 day delay, as shown in Fig. 3, where the DCF be-

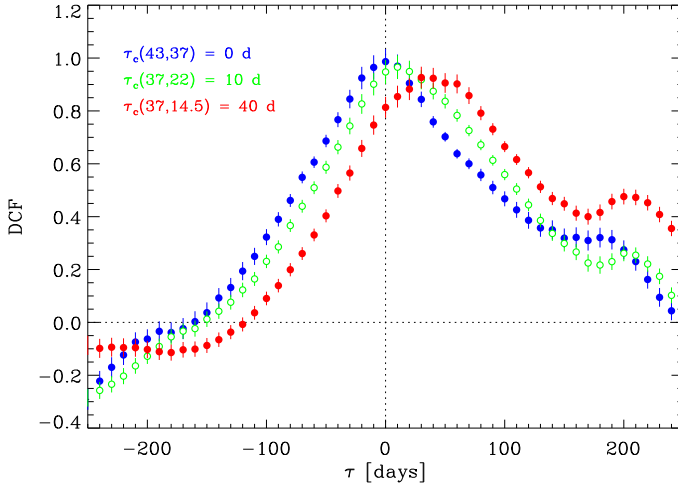


Fig. 2. Discrete correlation functions (DCFs) between radio light curves: 43 versus 37 GHz (blue filled circles), 37 versus 22 GHz (green empty circles), and 37 versus 14.5 GHz (red filled circles).

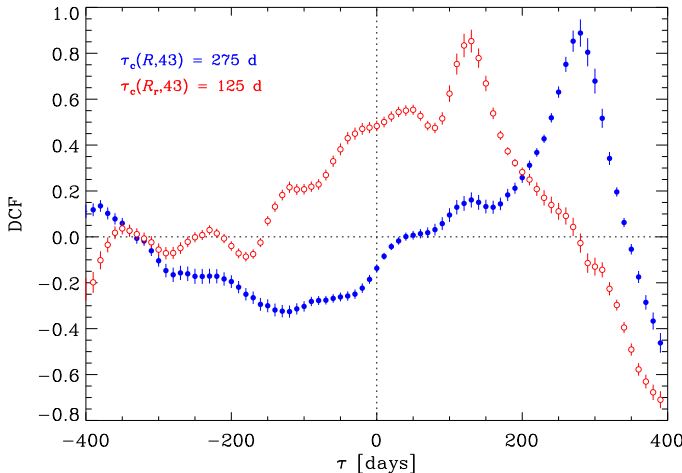


Fig. 3. Discrete correlation function (DCF) between the R -band and 43 GHz light curves (blue filled circles) compared with the DCF between the “rebeamed” R -band flux densities and the 43 GHz light curve (red empty circles; see text for details).

tween the 1-day binned R -band light curve and the 43 GHz spline is plotted as blue filled circles⁴.

This long time delay is not expected, especially in view of the fact that the millimetric outburst peaked around mid 2005, i.e. shortly after the optical one (Villata et al., 2006). Indeed, it is difficult to conceive why there should be such a little time delay (2–3 months) between the optical and mm variations, and such a large lag (about 9 months) between the optical and radio ones.

In fact, Villata et al. (2006) claimed that the outburst had fully propagated to the high radio frequencies by the end of September 2005, corresponding to the first hump of the 43 GHz light curve and implying an optical-radio delay of 4–5 months. Indeed, in the above optical-radio DCF (blue filled circles in Fig. 3) there is a little signal at about 130 days. This signal remains also when the DCF is calculated on the data after JD = 2453600

⁴ We chose the 43 GHz light curve instead of the better-sampled 37 GHz one because this latter misses an important feature like the first hump of the outburst mentioned in Sect. 2.1.

to exclude the optical outburst. Actually, it becomes the dominant one, even if faint ($DCF \sim 0.3$). It is due to the correlation between the minor optical flare peaking at JD ~ 2453670 (see top panel of Fig. 1) with the maximum peak of the 43 GHz light curve. In the following we thus consider the possibility that the 43 GHz maximum peak is not physically linked with the major optical outburst of spring 2005, but with the minor optical flare of October–November 2005.

3. Discussion and conclusions

Villata et al. (2006) suggested that the unprecedented luminosity of the spring 2005 optical outburst was mainly due to a decrease of the viewing angle of the optically emitting jet region, implying an increase of the beaming factor. In the same paper the authors argued also that the jet should present some bending, because of the lack of correlation between the historical optical and radio light curves. Hence, the radio outburst which followed after 4–5 months (first hump of the 43 GHz light curve) most likely occurred in a slightly misaligned outer region, so that the radio flux was not so enhanced as the optical one. At the time of the minor optical flare observed in October–November 2005 the jet must have turned, since the beaming of the optical radiation has decreased. On the other hand, the radio emitting region seems to have reached the minimum viewing angle at the time of the maximum peak.

This misalignment between the two regions makes the optical-radio cross-correlation analysis rather difficult. We thus investigate what happens when a correction for the misalignment is attempted, by simulating an optical light curve suffering beaming conditions comparable with the ones affecting the radio emission 130 days later, when the disturbances eventually reach the high-frequency radio emitting region (see Sect. 2.3).

The “true” optical flux densities F_R are transformed into “rebeamed”, simulated ones, F'_R , under the following assumptions: i) the observed flux density is proportional to δ^3 , where $\delta = [\gamma(1 - \beta \cos \theta)]^{-1}$ is the Doppler (beaming) factor and γ is the Lorentz factor⁵; ii) the minimum viewing angle θ_{\min} of the optically emitting region is achieved at $t = t_0$ for the “true” optical light curve, and at $t = t'_0$ in the case of the simulated one; iii) the viewing angle increases both forward and backward in time with the square root of the time elapsed since t_0 , $\theta(t) = \theta_{\min} + \sqrt{|t - t_0|/t_s}$, and similarly for the “rebeamed” case.

In the last but one panel of Fig. 1 we show the “rebeamed” optical light curve (grey and red dots) obtained with the model parameters set to: $\gamma = 10$, $\theta_{\min} = 5^\circ$, $t_0 = 2453490$, $t'_0 = 2453650$, $t_s = 14$ days⁶. Moreover, the simulated light curve has been shifted in time by 130 days in order to make the comparison with the 43 GHz spline easier. One can see that the general trend of the two light curves is quite similar, with the main difference that the 43 GHz variations appear to be smoother, as expected, since the radio emission is thought to come from a larger region. The result of their cross-correlation is shown in Fig. 3 as red empty circles, indicating a strong correlation with a radio delay of 125 days.

In other words, the radio delays come from the concomitance of two mechanisms acting on different time scales. The

⁵ We neglect here the minor Doppler effects on time intervals and frequencies.

⁶ While the resulting light curve is not very sensitive to changes in γ , θ_{\min} , and t_s , it is obviously strongly affected by the values of t_0 and t'_0 , which have been chosen close to the major (spring) and minor (autumn) optical events, respectively.

first mechanism is the perturbation travelling along the inhomogeneous jet, which causes the ~ 125 day radio lag. The other one is the “turning” of the curved jet, producing a differential variation of the viewing angle of the different emitting regions. This mechanism is responsible for the 275 day separation between the times of the optical and radio maximum beaming. In this framework the difference between the long delays of the radio outburst starting points and the shorter delays of the peaks discussed in Sect. 2.2 can be understood in terms of the different orientation of the radio emitting region at the times of the passage of the two perturbations, implying a greater contraction of the time scales when the viewing angle is smaller.

After the maximum peak, the radio flux drops rapidly at all the higher frequencies, and no flux enhancement is seen at the lower frequencies, as one would expect from the transit of the disturbance through outer regions. The reason may be that these jet regions are bent in such a way that the radiation emitted there is beamed elsewhere. Moreover, from the light curves in Fig. 1 one can see that the high-frequency radio spectrum is strongly inverted during the outbursts, suggesting that these events occurred inside the radio core, where low radio frequencies are still strongly absorbed. In other words, after mid 2006 the disturbances would be travelling in the misaligned jet region, i.e. out of the core (see the discussion by Bach et al. 2006 on the VLBA maps of BL Lacertae). Eventually they may become again visible when passing through outer regions having again a small viewing angle, and consequently appear as new radio components. Indeed, VLBA radio maps at 43 GHz taken in April and August 2006 do not show any new component yet, even if a slight elongation of the core in the jet direction is visible in the August map, i.e. towards the end of our observing period (Marscher et al., in preparation).

Finally, the above model can lead to a prediction for the behaviour of the millimetric emission in the same period. A reasonable hypothesis is that at these wavelengths the outburst development is intermediate between those observed in the optical and radio bands, with a first very strong mm outburst (as already reported by Villata et al. 2006), followed by a second, less prominent one. In the last panel of Fig. 1 the dotted line represents a sketch of the predicted 1 mm (230 GHz) light curve. It has been obtained as the average between the 43 GHz spline and a curve representing the optical data, shifted by 125 days. This latter curve is a cubic spline interpolation through the 15-day binned *R*-band flux densities, scaled as shown in the same panel to make them comparable with the radio ones. Then, the so obtained 1 mm curve has been normalized to have a maximum peak of about 40 Jy, and it has been shifted by 30 days back in time to make the peak occur in mid 2005, to match the observations quoted by Villata et al. (2006).

In summary, we are envisaging a scenario where the optically emitting region of a curved jet acquires its minimum viewing angle in spring 2005 (JD ~ 2453490), so that some disturbance(s) travelling in that region produces a maximally Doppler-enhanced outburst. Soon after also the mm region is affected by similar intrinsic (perturbation) and geometric (minimum viewing angle) conditions, even if this latter condition is probably reached with some delay. In the meanwhile some other perturbations (minor flares up to JD ~ 2453575 in the optical light curve) are crossing the optical region, which is becoming less and less well aligned with the line of sight. Most likely, some of these disturbances enter the mm region when it is still well oriented, thus producing a mm outburst more extended in time (probably more extended than in our toy-model prediction). The first disturbance is now crossing the 43–37 GHz region, followed

by the other ones. This train gives rise to the broad and modulated hump lasting about 250 days (JD ~ 2453500 –2453750). The lower-frequency emitting regions are also progressively perturbed. A new perturbation crosses the now misaligned optical region (flare around JD = 2453670), and produces a mild-intensity outburst when reaching the less misaligned mm region. Finally, it enters the high-frequency radio regions when their viewing angle is minimum, and it is Doppler-enhanced into an exceptionally bright event. All this happens in the VLBI radio core, where low frequencies are still well absorbed, and the outburst radio spectrum is strongly inverted. Only at the end of the outburst it gets softer, when the last disturbance leaves the highest-frequency radio regions.

Optical-to-radio monitoring by the WEBT is continuing to follow the source post-outburst phases.

Acknowledgements. We thank Alan Marscher for sharing useful information concerning changes in the VLBA images of 3C 454.3, and Philip Hughes for useful discussion. This work is partly based on observations made with the Nordic Optical Telescope, operated on the island of La Palma jointly by Denmark, Finland, Iceland, Norway, and Sweden, in the Spanish Observatorio del Roque de los Muchachos of the Instituto de Astrofísica de Canarias. It is partly based also on observations with the Medicina and Noto telescopes operated by INAF - Istituto di Radioastronomia. We thank the staff at the Medicina and Noto radio observatories for their help and support during the observations. This research has made use of data from the University of Michigan Radio Astronomy Observatory, which is supported by the National Science Foundation and by funds from the University of Michigan. This work was partly supported by the Italian Space Agency (ASI) under contract ASI/INAF I/023/05/0. The St. Petersburg team acknowledges support from Russian Federal Program for Basic Research under grant 05-02-17562. RATAN-600 observations were partly supported by the Russian Foundation for Basic Research grant 05-02-17377. This project was done while YYK was a Jansky fellow of the National Radio Astronomy Observatory and a research fellow of the Alexander von Humboldt Foundation.

References

Bach, U., Villata, M., Raiteri, C. M., et al. 2006, A&A, 456, 105
 Edelson, R. A. & Krolik, J. H. 1988, ApJ, 333, 646
 Fuhrmann, L., Cucchiara, A., Marchili, N., et al. 2006, A&A, 445, L1
 Giommi, P., Blustin, A. J., Capalbi, M., et al. 2006, A&A, 456, 911
 Hufnagel, B. R. & Bregman, J. N. 1992, ApJ, 386, 473
 Peterson, B. M. 2001, in Advanced Lectures on the Starburst-AGN Connection, ed. I. Artxaga, D. Kunth, & R. Mújica (Singapore: World Scientific), 3
 Pian, E., Foschini, L., Beckmann, V., et al. 2006, A&A, 449, L21
 Raiteri, C. M., Villata, M., Ibrahimov, M. A., et al. 2005, A&A, 438, 39
 Raiteri, C. M., Villata, M., Kadler, M., et al. 2006, A&A, 459, 731
 Raiteri, C. M., Villata, M., Tosti, G., et al. 2003, A&A, 402, 151
 Villata, M., Raiteri, C. M., Aller, H. D., et al. 2004a, A&A, 424, 497
 Villata, M., Raiteri, C. M., Balonek, T. J., et al. 2006, A&A, 453, 817
 Villata, M., Raiteri, C. M., Kurtanidze, O. M., et al. 2004b, A&A, 421, 103

List of Objects

‘3C 454.3’ on page 1
 ‘3C 454.3’ on page 1
 ‘3C 454.3’ on page 1
 ‘3C 454.3’ on page 2